HHS Public Access

Author manuscript

Circulation. Author manuscript; available in PMC 2018 March 28.

Published in final edited form as:

Circulation. 2017 March 28; 135(13): 1240–1252. doi:10.1161/CIRCULATIONAHA.116.024826.

AUGMENTATION OF MUSCLE BLOOD FLOW BY ULTRASOUND CAVITATION IS MEDIATED BY ATP AND PURINERGIC SIGNALING

J. Todd Belcik, BS, ACS, RDCS[1], **Brian P. Davidson, MD**[1], **Aris Xie, MS**[1], **Melinda D. Wu, MD**[3], **Mrinal Yadava, MD**[1], **Yue Qi, MD**[1], **Sherry Liang, MS**[1], **Chae Ryung Chon**[1], **Azzdine Y. Ammi, PhD**[1], **Joshua Field, MD**[4], **Leanne Harmann, RDCS**[4], **William M. Chilian, PhD**[5], **Joel Linden, PhD**[6], and **Jonathan R. Lindner, MD**[1,2]

[1]Knight Cardiovascular Institute, Oregon Health & Science University, Portland, OR

[2]Oregon National Primate Research Center, Oregon Health & Science University, Portland, OR

[3]Doernbecher Children's Hospital, Portland, OR

[4]Division of Hematology and Oncology, Medical College of Wisconsin, Milwaukee, WI; and Blood Center of Wisconsin, Madison, WI

[5]Northeast Ohio Medical University, Rootstown, OH

[6]Division of Development Immunology, La Jolla Institute for Allergy and Immunology, and Department of Pharmacology, University of California San Diego, San Diego, CA

Abstract

Background—Augmentation of tissue blood flow by therapeutic ultrasound is thought to rely on convective shear. Microbubble contrast agents that undergo ultrasound-mediated cavitation markedly amplify these effects. We hypothesized that purinergic signalling is responsible for shear-dependent increases in muscle perfusion during therapeutic cavitation.

Methods—Unilateral exposure of the proximal hindlimb of mice (with or without ischemia produced by iliac ligation) to therapeutic ultrasound (1.3 MHz, mechanical index 1.3) was performed for ten minutes after intravenous injection of 2×10^8 lipid microbubbles. Microvascular perfusion was evaluated by low-power contrast ultrasound perfusion imaging. In vivo muscle ATP release and in vitro ATP release from endothelial cells or erythrocytes were assessed by a luciferin-luciferase assay. Purinergic signalling pathways were assessed by studying interventions that either (1) accelerated ATP degradation; (2) inhibited P2Y receptors, adenosine receptors, or K_{ATP} channels; or (3) inhibited downstream signalling pathways involving endothelial nitric oxide synthase (eNOS) or prostanoid production (indomethacin). Augmentation in muscle perfusion by ultrasound cavitation was assessed in a proof-of-concept clinical trial in 12 subjects with stable sickle cell disease (SCD).

Address correspondence to: Jonathan R. Lindner, MD, Knight Cardiovascular Institute, Oregon Health & Science University, 3181 SW Sam Jackson Park Rd., Portland, OR 97239, Tel. (503) 494-8750, Fax (503) 494-8550, lindnerj@ohsu.edu.

DISCLOSURES

There are no disclosures or conflicts of interest related to this study.

Results—Therapeutic ultrasound cavitation increased muscle perfusion by 7-fold in normal mice, reversed tissue ischemia for up to 24 hrs in the murine model of peripheral artery disease, and doubled muscle perfusion in patients with SCD. Augmentation in flow extended well beyond the region of ultrasound exposure. Ultrasound cavitation produced a nearly 40-fold focal and sustained increase in ATP, the source of which included both endothelial cells and erythrocytes. Inhibitory studies indicated that ATP was a critical mediator of flow augmentation that acts primarily through either P2Y receptors or through adenosine produced by ectonucleotidase activity. Combined indomethacin and inhibition of eNOS abolished the effects of therapeutic ultrasound, indicating downstream signalling through both NO and prostaglandins.

Conclusions—Therapeutic ultrasound using microbubble cavitation to increase muscle perfusion relies on shear-dependent increases in ATP which can act through a diverse portfolio of purinergic signalling pathways. These events can reverse hindlimb ischemia in mice for >24 hours, and increase muscle blood flow in patients with sickle cell disease.

Clinical Trial Registration—NCT01566890 (https://clinicaltrials.gov/ct2/show/NCT01566890)

Keywords

contrast echocardiography; microbubbles; microcirculation; perfusion

Journal Subject Terms

Ultrasound; Peripheral Vascular Disease; Ischemia; Vascular Biology

---

Distribution of blood flow in the body is tightly regulated to meet tissue metabolic and functional demand. Vascular conductance is determined primarily by microvascular tone which is in part under the regulatory control of vasoactive substances that change according to metabolic substrate needs, pH, temperature, pressure, and shear.[1–3] Mechanistic knowledge of vasomotor control has been critical for developing therapies for hypertension, shock, tissue ischemia, and heart failure; most of which rely on pharmacologic mimicry or modification of endogenous vasoactive substances. Shear-dependent vasodilation is a response mediated by endothelial-derived substances and is permissive for lowering vascular resistance in response to downstream hyperemia and for reducing cardiac work during exercise based on how the radii of a branching tube system influences the energy of flow delivery.[2,4]

Ultrasound (US) is increasingly used for a wide variety of therapeutic applications, some of which rely on US-mediated effects on perfusion. Vasodilation in large vessels and the microcirculation occurs in response to US over a wide frequency range and is thought to be secondary to oscillatory pressures or vascular shear produced by convective motion.[5,6] The presence of gas bodies within the microcirculation in the form of encapsulated microbubble contrast agents that undergo acoustic cavitation can produce very high focal shear and markedly augment the effects of US on blood flow.[7,8] Contrast-enhanced ultrasound (CEU) with microbubbles is being investigated as a promising therapy for acute ischemic syndromes.

With regards to the mechanism for flow augmentation during US cavitation, a direct coupling between US-mediated shear and NO release has been proposed previously.[6,9,10] In this study we sought to investigate other key molecular pathways, including ATP release which is known to influence blood flow through a combination of mechanisms that include conversion to adenosine and calcium-dependent endothelial purinergic receptor signaling that secondarily activates endothelial nitric oxide synthase (eNOS) and release of prostaglandin-derived vasodilators. We also sought to investigate whether US cavitation can reverse tissue ischemia in a murine model of chronic hindlimb ischemia, and increase skeletal muscle blood flow by in patients with sickle cell disease (SCD), a disease where abnormalities in perfusion are attributable in part to impaired endothelial-dependent vasoactive pathways.[11]

METHODS

Animal Models

The study was approved by the Animal Care and Use Committee of the Oregon Health & Science University. Wild-type C57Bl/6 mice and P2Y2$^{-/-}$ mice (*P2ry2*^{tm1Bhk}/J) on a 129P2 background were obtained from Jackson Laboratory. Mice were studied at 10–20 weeks of age. Mice were anesthetized for study procedures with inhaled isofluorane (1.0–1.5%) mixed with room air and kept euthermic with external heating sources. For CEU studies, a jugular vein was cannulated for intravenous access. The unilateral hindlimb ischemia model was produced by ligation of the distal common iliac artery and the origin of the epigastric artery through a midline abdominal incision using sterile technique, after which mice were recovered and buprinorphine HCL (0.2 mg/kg IM) was administered for analgesia. Mice were restudied 20–25 days after surgical ligation to allow for completion of endogenous angiogenic responses.

Pathway Inhibition in Mice

Vasoactive signaling pathways were inhibited mice with the following protocols that have been previously validated. Inhibition of eNOS was performed with 75 μg/kg L-nitroarginine methyl ester (L-NAME, Santa Cruz Biotech., Santa Cruz, CA) given IP 30 min prior to study. Blockade of adenosine A_2-receptors was performed with 50 μg/g of 4-(2-[7-Amino-2-(2-furyl)[1,2,4]triazolo[2,3-a][1,3,5]triazin-5-ylamino]ethyl)phenol (ZM-241385, Abcam PLC, Cambridge, MA) given IV 1 hr prior to study. This dose is predicted to inhibit both A_{2a} and A_{2b} receptors. Accelerated metabolism of ATP was performed with 4.0 U/g apyrase (Sigma-Aldrich, St. Louis, MO) given IP 1 hour prior to study; while inhibition of ectonucleotidases involved in ATP metabolism was performed by 1 μg/g of sodium polytungstate (POM-1, VWR, Radnor, PA) given by IP injection 30 min prior to study. For inhibition of the K_{ATP} receptor was performed by 15 mg/kg glibenclamide (Santa Cruz Biotechnology, Dallas, TX) given IV 30 min prior to study. For inhibiting intracellular signaling pathways, L-NAME (20 mg/kg) was administered by IV route 10 min prior to imaging; and indomethacin (2 mg/kg) was given by IP route 24 hrs and again 1 hr prior to study.

Microbubble Preparation

See online Supplement.

Murine Therapeutic Ultrasound Protocols

The proximal adductor muscles of the left hindlimb were exposed to therapeutic US for 10 min. A phased-array transducer was placed at a fixed distance (3 cm) from the mid-portion of the muscle using a transverse imaging plane and US was performed over 10 min using harmonic power-Doppler imaging (Sonos 7500, Philips Ultrasound, Andover, MA) at 1.3 MHz triggered at 5 s intervals. For these pulses, a pulse repetition frequency of 9.3 kHz, and a mechanical index (MI) of 1.3. Microbubbles (2×10^8) were suspended in ≤200 μL of normal saline and administered over the first minute of ultrasound exposure.

Cavitation Detection

See on-line Supplement

Murine Microvascular Perfusion Imaging

Contrast-enhanced ultrasound perfusion imaging of the proximal hindlimb adductor muscles of the therapeutic ultrasound-exposed and contralateral control limb was performed 10 min after therapeutic US. The non-linear fundamental signal component from MBs was detected using multipulse phase-inversion and amplitude-modulation (Sequoia 512, Siemens Medical Systems, Mountain View, CA) at 7 MHz and an MI of 0.18 with a linear-array transducer. This form of low-power imaging has been shown not to produce any detectable changes in perfusion.[8] Microbubbles were infused at a rate of 1×10^7 min^{-1}. Time-intensity data at a frame rate of 5 Hz were acquired after a high-power (MI 0.98) 5-frame sequence and were fit to the function: $y=A(1-e^{\beta t})$; where y is intensity at time t, A is the plateau intensity representing relative microvascular blood volume, and the rate constant β is the microvascular flux rate.[12] Microvascular blood flow (MBF) was quantified by the product of A and β.[12]

Spatial Assessment of Flow Augmentation

The spatial extent of US cavitation-mediated increases in perfusion beyond the boundaries of the therapeutic US transducer was assessed. After completing therapeutic US cavitation in the short-axis plane of the hindlimb in mice, the location of the beam was marked and the diagnostic linear-array transducer was aligned in the long-axis (90° rotation from the therapeutic probe orientation). Microbubbles were infused at a rate of 1×10^7 min^{-1} and maximum intensity projection imaging using settings described above for perfusion imaging was performed for a 6 second acquisition after a high power destructive pulse sequence at an MI of 0.98. Intensity was measured from within the therapeutic sector plane and at incremental distances (2, 4, and 6 mm) beyond the sector plane at 1, 3 and 6 seconds of MIP acquisition. Since flow augmentation was manifest primarily as an increase in β, the primary outcome measure on MIP was the regional intensity at the shortest (1 s) acquisition duration.

Ex Vivo Arterial Dilation

See online Supplement.

In vivo Imaging of ATP Release

Optical imaging of luciferin-luciferase activity was performed to temporally and spatially assess intravascular ATP release. Mice were injected IP with 3 mg D-luciferin (Thermo Fisher, Waltham, MA) by IP route immediately before therapeutic US with MB cavitation. Firefly luciferase (25 μg, Thermo Fisher) was injected by IV route 1 min prior to completion of the 10 min US exposure. Optical imaging (IVIS Spectrum, Caliper Life Sciences) was performed at 5, 10, 15, and 20 min after completion of US using medium binning. Repeat injections of D-luciferin and luciferase were repeated 24 hrs later. Data were expressed as photons/s/cm^2.

Endothelial Cell and Erythrocyte ATP Release

Murine endothelial cells (SVEC4-10, ATCC, Manassas, VA) were grown to confluence in DMEM supplemented with 10% fetal bovine serum in 75 mm culture flasks. Immediately prior to study, DMEM was exchanged to capacity with fresh medium at 37° C containing 0.5 mg D-luciferin, 5 μg firefly luciferase, and 5×10^8 MBs. Optical imaging was performed after exposure to US for 1 min at frame rate of 1 Hz otherwise using the same settings as the murine experiments except. Human RBCs were obtained from normal volunteers, washed, and 1 mL was diluted 1:34 with DMEM containing 0.5 mg D-luciferin, 5 μg firefly luciferase, and 5×10^8 MBs prior to US exposure. Combination experiments were performed with both RBCs and SVEC4-10 endothelial cells; and control experiments were performed without US but with a matched 1 min delay in imaging. For each condition, results from 6 experiments were averaged. In order to evaluate for persistent ATP release (i.e. mechanotransduction) after resolution of microporation (see below), experiments with endothelial cells were repeated with a 20 min delay in adding D-luciferin and luciferase. For these experiments, DMEM exchange was performed 15, 10 and 1 min prior to adding luciferin and luciferase. Control experiments with DMEM exchange were also performed.

Assessment of Cellular Poration

See on-line Supplement

RBC deformability

See on-line Supplement

Muscle eNOS Phosphorylation

Phosphorylation of eNOS at Ser1177 was evaluated in muscle samples obtained from within the ultrasound imaging sector and from non-exposed muscle. Samples were obtained within 15 min of completion of US exposure. For enzyme-linked immunosorbent assay (ELISA), bilateral hindlimb muscle samples were obtained from 9 wild-type mice, 5 $P_2Y_2^{-/-}$ mice, and 6 $P_2Y_2^{-/-}$ mice treated with ZM-241385. Samples were homogenized in lysis buffer containing 1mM phenylmethylsulfonyl fluoride, centrifuged, and the supernatant was evaluated for phosphorylated eNOS using an (PathScan ELISA, Cell Signaling Tech.).

Assessment of Flow Augmentation in Patients with SCD

The study was approved by the Institutional Review Board of the Medical College of Wisconsin. Twelve African American subjects with SCD (18±4 yrs of age; 4 males and 8 females) were studied. All subjects had a history of SCD (S/S HbB phenotype). Exclusion criteria included vaso-occlusive crisis within the prior 3 months, heart failure, significant right-to-left shunt, and allergy to ultrasound contrast agent. Therapeutic US cavitation and microvascular perfusion imaging were performed simultaneously using a protocol where MB replenishment kinetics are evaluated from the progressive prolongation of high-power destructive pulse sequences.[12] The proximal forearm flexor muscles (flexor digitorum superficialis and profundus) were imaged in the transverse plane approximately 1/3 the distance to the wrist using a phased-array transducer interfaced with an ultrasound system (iE33, Philips Ultrasound). Power modulation imaging was performed using a broad-band pulse centered at 2.0 MHz at a mechanical index of 1.0 with the acoustic focus placed at the mid-muscle level. One vial of lipid-shelled octafluoropropane MBs (Definity, Lantheus Medical Imaging, N. Billerica, MA) was diluted to a total volume of 30 mL in 0.9% saline for a final concentration of 5×10^8 mL^{-1}. The MB suspension was infused intravenously at 1.5 mL/min. Imaging was started after allowing MB concentration to come to steady state (approximately 2 min). A short (2–3 s) continuous imaging sequence was followed by acquisition of intermittent frames obtained at incrementally increasing time intervals from every 1 to 15 cardiac cycles at end-diastole by gating acquisition to the electrocardiographic R-wave. Several frames were acquired for each pulsing interval. The total time of acquisition was approximately 3–4 min. This process was repeated three times over a total duration of 15 min or less. Progressive prolongation of the pulsing interval guaranteed exposure of MBs to US within the entire span of the muscle circulation and also allowed quantification of perfusion. For the latter, several continuous imaging frames were averaged and digitally subtracted from averaged frames at each pulsing interval. Time versus background-subtracted video intensity data from the muscle were fit to the function: $y=A(1-e^{\beta t})$; where y is intensity at time t, A is the plateau intensity representing relative microvascular blood volume, and the rate constant β is the microvascular flux rate.[12] Microvascular blood flow (MBF) was quantified by the product of A and β.[12] The effect of MB cavitation was evaluated by comparing data from the first US prolongation sequence (0–5 min) to the third sequence (10–15 min).

Statistical Analysis

Data were analyzed using Prism (version 5.0, GraphPad Software). Group-wise differences were assessed by Mann-Whitney U test for data that were determined to be non-normally distributed by D'Agostino and Pearson omnibus test. For data with normal distribution, group-wise differences were assessed by one-way ANOVA with post-hoc unpaired Student's t-test and Bonferroni's correction when evaluating different testing conditions; and paired Student's t-test when comparing limbs exposed to ultrasound to control contralateral limbs. Differences were considered significant at $p<0.05$ (2-sided).

RESULTS

US results in immediate and sustained extracellular ATP release

We first quantified the increase in limb muscle blood flow created by US-mediated cavitation in anesthetized adult C57Bl/6 mice undergoing US (1.3 MHz, mechanical index 1.3) delivered at a pulsing interval of 5 sec with a phased-array transducer placed over the left proximal hindlimb adductor muscle group. Ultrasound was performed for 10 min after a single intravenous injection of lipid-shelled decafluorobutane-core microbubbles with a composition, zeta potential, and size distribution similar to that for certain commercially-produced microbubble agents (Supplemental Fig. 1). These ultrasound powers which are within the diagnostic range do not produce significant adverse bioeffects, but did generate inertial cavitation energy *in vivo* detected by broad-band signal which indicates high shear ultrasound events in the vascular compartment(Fig. 1a). After high-power US exposure, CEU perfusion imaging performed at very low power which has no effects on tissue blood flow[8] revealed a 6-fold increase in perfusion in the muscle exposed to US (Fig. 1b to f). This increase in perfusion was attributable mainly to an increase in the microvascular blood flux rate (β), with little increase in microvascular blood volume, which is an index of the number of microvascular units perfused. Re-orientation of the probe to assess perfusion in the limb long-axis was performed together with maximum-intensity projection imaging to evaluate the spatial distribution of flow after high-power therapeutic US,[13] which demonstrated flow augmentation throughout the entire proximal hindlimb (Supplemental Fig 2) However, the hyperemic response was greatest in the region exposed to high-power therapeutic US (Fig. 1g and h, Supplemental Fig 3).

Microstreaming during ultrasound-induced cavitation of microbubbles produces focal shear stress that can be orders of magnitude greater than that produced by physiologic flow.[14] Because extracellular ATP derived from both endothelial cells and red blood cells (RBCs) is recognized as an important biologic mediator of shear-dependent vasodilation,[15–18] we investigated the temporal release of ATP within the vascular compartment after US cavitation. *In vivo* optical imaging was performed in anesthetized mice receiving intraperitoneal *d*-luciferin 10 min before US, and intravenous firefly luciferase 1 min prior to completing US exposure. Photon flux from the ATP-dependent luminescent reaction was 40-fold higher in the US-exposed versus contralateral control hindlimb early after exposure (Fig. 1i and j). Focal ATP signal in the US-exposed limb decreased gradually over time and, although greatly attenuated by 24 hrs was still 5-fold greater (p=0.03) than in the contralateral non-exposed limb.

Flow augmentation with US cavitation is mediated by ATP

Because US cavitation produced immediate and sustained increases in ATP release, we examined whether US-mediated augmentation of perfusion was affected by modifying vasoactive pathways mediated by ATP. Membrane-bound and soluble ectoucleotides including nucleoside triphosphate diphosphohydrolases (NTPDase) of the CD39 family degrade ATP and ADP to AMP, while ecto-5′-nucleotidase (CD73) degrades AMP to adenosine.[18–20] These enzymes have been shown to also be released in response to shear.[18] Adenosine produces vasodilation mostly through Gs-coupled A_{2A} or A_{2B} on smooth muscle

cells, or on endothelial cells where vasodilation is mediated in part by phosphorylation and activation of eNOS.[21–23] As a first step to investigate the roles of adenosine and ATP, mice undergoing US-mediated cavitation of the hindlimb were pretreated with the A_2 receptor antagonist ZM241385, or the ectonucleotidase (CD39) inhibitor sodium polyoxotungstate (POM-1).[24] Adenosine receptor blockade alone had no significant effect on muscle perfusion, whereas POM-1 modestly reduced both microvascular flux rate and blood flow (Fig. 2a and Supplemental Fig. 4).

Direct ATP signaling through endothelial G-coupled P_2Y purinergic receptors has been shown to produce vasodilation in skeletal muscle and mesenteric microcirculation, albeit with less of an effect in the coronary circulation.[16,25–27] Accordingly, we investigated the role of direct ATP signaling in US-mediated augmentation of perfusion. Administration of apyrase as an exogenous CD39-like nucleotidase that rapidly degrades ATP did not change blood flow response to US cavitation (Fig. 2a and Supplemental Fig. 4). We then tested the possibility that *both* the P_2Y and adenosine pathways could be mutually compensatory with regards to their vasodilatory effects (i.e. ability to shuttle between the pathways) by two separate approaches. First, wild-type mice were pre-treated with both apyrase to promote ATP degradation and ZM241385 to inhibit adenosine A_{2A} and A_{2B} receptors, the latter of which has been shown alone to not influence flow augmentation.[8] Second, mice deficient for the major P_2Y endothelial receptor in skeletal muscle microvasculature ($P2Y_2^{-/-}$) were studied after treatment with ZM241385. These two approaches resulted in a similar and substantial reduction in perfusion in the US-treated limb (Fig 2a and Supplemental Fig 4), indicating that vasodilation in response to US-mediated cavitation is largely mediated by a combination of purinergic pathways. Because activation of endothelial or smooth muscle K_{ATP} channels via ATP efflux represents an alternative pathway by which adenosine can mediate vasodilation,[21] we investigated the effect of receptor blockade with glibenclamide which was found not to have a major effect on US cavitation-mediated augmentation in flow (Fig. 2b, Supplemental Fig. 4).

Because our data indicated that augmentation in perfusion from US cavitation is mediated in part through the endothelial $P2Y_2$ receptor, we investigated the signaling pathways that are thought to mediate the vasoactive effects of P_2Y receptor activation, including calcium-dependent phosphorylation of eNOS, and phospholipase-A2-mediated production of vasoactive arachidonic acid metabolites.[16,28–30] Skeletal muscle from wild-type mice that had been exposed to US-induced microbubble cavitation demonstrated significant increases in phosphorylated eNOS by ELISA (Fig. 2c). Because eNOS phosphorylation can occur via alternative non P2Y-receptor-mediated processes that include K_{ATP} and A_{2B} receptor activation, H_2O_2, and other endothelial-derived hyperpolarizing factors;[21,22,31] we also evaluated phospho-eNOS in $P2Y_2^{-/-}$ mice with and without inhibition of adenosine receptors. In these animals, cavitation-mediated phosphorylation of eNOS was lower than in wild-type mice to a similar degree (Fig. 2c). To investigate the functional significance of inhibiting both the eNOS and arachidonic acid pathways downstream from P_2Y activation, wild-type mice were pre-treated with the eNOS inhibitor L-N^G-nitroarginine methyl ester (L-NAME) or indomethacin. Each of these interventions decreased flow augmentation produced by US cavitation, whereas the combination of the two essentially abolished flow augmentation. (Fig. 2d and Supplemental Fig. 4).

In aggregate, our data indicate the ATP is critical mediator of flow augmentation produced by ultrasound cavitation and can act either through P2Y receptor signaling or through adenosine produced by ectonucleotidase activity.

Cell Source for Cavitation-mediated ATP Release

Whereas US alone influences pressure and shear conditions of all cell types within the acoustic field, the augmentation of shear-mediated effects with microbubble cavitation is limited to focal regions within the vascular space where microbubbles are confined.[32] Both endothelial cells and RBCs are in close proximity to microbubbles and both release ATP in response to shear.[15,17,18,33] We used an extracellular luciferin-luciferase assay to quantify ATP release from cultured microvascular endothelial cells (SVEC4-10 derived from SV40 transformation), human RBCs, or a combination of the two. These studies demonstrated immediate release of ATP from both cell types after exposure to US-mediated microbubble cavitation (Fig. 3a and b). The functional impact of RBCs was further investigated by assessing vascular response in a perfused *ex vivo* microvascular preparation. The diameter of rat mesenteric arteries increased incrementally with sequential ultrasound exposure of MBs without and with RBCs (40% volume) (Supplemental Fig. 5).

Potential mechanisms for this finding include mechanotransduction with the opening of shear-dependent ATP channels that have been identified on RBCs and endothelial cells such as pannexins,[15,34,35] or transient (<10 min) microporation that can occur with microbubble cavitation.[36] The extent and duration of endothelial cell microporation was assessed by nuclear DNA fluorescence from propidium iodide (PI) which is normally excluded by intact cell membranes. PI was added to the culture medium of untreated cells or to cells at the time of US exposure, or 10 or 20 min after exposure. Nuclear PI fluorescence was seen in the vast majority of cells when PI was ambient at the time of US cavitation, but only in approximately 15–20% of cells when PI was added at 10 or 20 min after US (Fig. 3c and d). These data indicate cavitation-mediated microporation of most cultured cells as a potential contributor to ATP release with permanent loss of viability (indicated by late PI staining), in only a small percentage. To investigate for sustained ATP release by mechanotransduction after resolution of microporation, optical imaging after US cavitation was repeated with a 20 min delay in adding luciferin-luciferase to endothelial cells with several interval low-shear medium exchanges. Persistent ATP release was detected after allowing time for resolution microporation (Fig. 3e), which is consistent with mechanotransduction as a second mechanism and serves to explain the sustained local *in vivo* ATP release detected as late as 24 hours after US (Fig. 1i and j). We confirmed that RBCs also undergo transient microporation similar to that seen for endothelial cells by using flow cytometry which detected positive fluorescent staining of RBCs after exposure to US cavitation in the presence of Texas red-labeled dextran (Fig. 3f). There was a reduction of the proportion of cells with positive fluorescent staining with increasing time between US cavitation and the addition of labeled dextran. To ensure that ATP release from RBCs did not influence their deformability which has a major influence on relative effective viscosity and resistance at the capillary level,[37] laser-assisted RBC deformability measurements were made and confirmed no effect from cavitation (Fig. 3g).

US cavitation as therapy

The ability to almost immediately increase skeletal muscle perfusion with US cavitation represents a potential therapy for rapidly reversing limb ischemia in subjects with limb ischemia due to severe peripheral artery disease (PAD). To examine the effect of US cavitation on ischemic limb perfusion, a murine model of chronic PAD was produced by ligation of several major limb inflow vessels to produce moderate ischemia.[38] Because hypoxia is a recognized stimulus for ATP release from RBCs,[39,40] we first performed *in vivo* optical imaging to examine whether US cavitation stimulates ATP release in the setting of chronic ischemia. Focal ATP release was seen at the site of US exposure (Fig. 4a and b) albeit to a lesser extent than that seen in the non-ischemic setting. We then examined the ability of US cavitation to reverse limb ischemia in the murine model. These studies demonstrated augmentation of perfusion in the ischemic hindlimb to a degree that was higher than in the control non-ischemic contralateral limb early after US exposure and similar to that in the control non-ischemic limb at 24 hrs (Fig. 4c and d). Again, the beneficial vascular effect extended distally in the limb beyond the area exposed to therapeutic US (Supplemental Fig. 6).

To investigate the beneficial effects of US cavitation on perfusion in humans, we studied patients with SCD in whom an imbalance in vasoactive intermediates contributes to pathophysiology.[11] There are also data suggesting that hydroxyurea, a commonly used treatment for SCD, produces NO-mediated vasodilation in part through RBC release of ATP.[41] Accordingly, in 12 patients with SCD not in vaso-occlusive crisis, US (1.3 MHz) was applied to the proximal forearm at a mechanical index of 1.3 during intravenous administration of lipid-shelled octafluoropropane microbubbles. In these experiments therapeutic and diagnostic perfusion imaging were simultaneously performed by progressive prolongation of the interval between US frames from every 1 to 15 cardiac cycles which allowed for both construction of time-intensity curves and high-power exposure of MBs to US at various levels of the microcirculation. Three separate acquisitions (3 min exposure) were performed at approximately 5 min intervals. Muscle perfusion in the flexor digitorum superficialis and profundus increased on average by 2-fold between the first US exposure (at 0–5 min) and the final US exposure (10–15 min) (Fig. 4e). This cavitation-mediated increase in perfusion was attributable primarily to an increase in microvascular blood flux rate (β) (Fig. 4f – 4h).

DISCUSSION

Therapeutic US over a wide range of frequencies and pressures is currently used for treating a wide range of diseases. High-intensity and highly-focused US is widely used in patients for tissue ablative therapy such as for benign or malignant tumors or renal calculi. The non-thermal bioeffects responsible for ablative therapy include cavitation events that disrupt tissue through shear produced by microstreaming and shock wave. Non-thermal shear forces are thought to also participate in the beneficial effects of lower amplitude US on tissue healing and blood flow.

Gas bodies in the form of membrane-stabilized microbubble contrast agents, including those that have undergone regulatory approval for diagnostic applications, act as cavitation nuclei

within the microcirculation and have been shown to amplify US-mediated augmentation of perfusion.[8,42] For limb perfusion, pre-clinical studies have demonstrated that addition of microbubbles to ultrasound alone results in a >5-fold greater effect on muscle blood flow and a greater increase in arterial dilation.[8] The effects of CEU on perfusion are greatest when the acoustic power is high enough to produce inertial cavitation (exaggerated microbubble oscillation and destruction), and there is also sufficient time between ultrasound exposures to allow refill of microbubbles into the ultrasound sector.[8] These findings indicate that focal intense increases in shear caused by cavitation events that occur infrequently (every 5 seconds in this study) and sparsely within the microcirculation are more effective at increasing vascular conductance than exposure of the entire microcirculation devoid of MBs to continuous US energy.[8] Although speculative, a potential explanation for this finding is that vascular effects may occur remotely from the site of cavitation since both focal mechanical stress and ATP release produce propagated calcium waves to activate endothelial cell networks.[43,44]

The biophysical events produced by MB cavitation have been shown to initiate cellular responses known to be important in the regulation of vascular tone. Cavitation-mediated increases in endothelial NO production and intracellular calcium have been described and have been attributed to activation of vaguely-defined endothelial shear mechanotransducers or to transient membrane microporation.[6,8,9,45] In this study, we have defined a multi-faceted pathway (schematically illustrated in Fig. 5) by which cavitation increases microvascular perfusion and that is not simply from direct mechanotransductive activation of eNOS. Cavitation produces a large ATP release from both endothelial cells and RBCs. The temporal pattern of this release suggests that an immediate phase from microporation is followed by sustained release that likely reflects either previously described shear-sensitive opening of ATP channels such as pannexin 1 or ATP-mediated ATP release.[15,34,44] Based on our varied manipulations of potential vasoactive pathways, it appears that the mechanism for flow augmentation can be “shuttled” between either P2Y receptor activation, or ecto-nucleotidase degradation of ATP to adenosine. There was no major contribution from K_{ATP} receptor activation. Irrespective of which receptor pathway was stimulated, the downstream events involve both activation of eNOS and production of prostanoids such as prostacyclin presumably downstream from calcium-dependent PLA_2 activity.[16,21,30]

The mechanistic insights from this study are important for several reasons. They are important for understanding how to optimize cavitation for therapeutic benefit beyond the preliminary observations that we have performed in mice with limb ischemia and patients with SCD. The ability to increase tissue perfusion in a highly targeted fashion could be important for improving symptoms in chronic ischemic coronary and peripheral artery disease, for reversing acute ischemic emergencies (e.g. stroke, acute coronary syndrome, threatened limb loss), for improving tissue-specific functions that rely on adequate perfusion (e.g. renal and pancreatic function, tissue healing), or even possibly for treating Alzheimers.[46] From a diagnostic standpoint, provocative non-invasive tests for assessing shear-mediated flow augmentation could provide a robust approach for assessing endothelial health. Currently, non-invasive assessment of endothelial health commonly involves the measurement of very small changes in large arterial diameter that are produced during post-occlusive hyperemia.

The discovery of ATP as a mediator of cavitation-mediated augmentation in perfusion together with observation of flow augmentation outside of the region of cavitation serves as an applied example of how focal mechanical events can lead global microvascular network response. We presume that this response reflects calcium wave propagation which can be mediated by ATP release.[44] Finally, downstream effects from ATP signaling are likely to contribute to other therapeutic uses of US such as for drug or gene delivery and tissue healing that are thought to rely on calcium-dependent uptake.

There are several limitations of this study that must be acknowledged. Dose response in terms of ultrasound energy, frequency, or duration was not performed with regards to ATP release. Instead, we used ultrasound parameters which we have previously demonstrated to produce a marked increase in limb perfusion and which do not produce any unwanted adverse bioeffects such as microvascular hemorrhage.[8,47] In these previous studies, flow augmentation was dose-dependent with regards to MB dose and ultrasound power. An important limitation is that we have not yet identified the channel or other mechanism responsible for the sustained phase of ATP release. The models necessary for evaluating ATP release mechanism are not yet available to us for study. It should also be acknowledged that the clinical trial in patients with SCD was performed as a “proof-of-concept” study without rigorous attention to optimization of power, microbubble dose, or field exposure.

In conclusion, in this study we have demonstrated that increased vascular conductance from ultrasound cavitation is mediated by a diverse portfolio of calcium-dependent ATP signalling pathways including endothelial purinergic P2Y-receptor activation and extracellular conversion of ATP to adenosine. Both of these pathways acted through endothelial nitric oxide synthase and production of vasoactive prostanoids. These vascular effects of ultrasound cavitation can reverse hindlimb ischemia in mice for >24 hours, and increase skeletal muscle blood flow by approximately 2-fold in patients with sickle cell disease.

Supplementary Material

Refer to Web version on PubMed Central for supplementary material.

Acknowledgments

SOURCES OF FUNDING

Dr. Lindner is supported by grants R01-HL078610, R01-HL111969 and R01-HL120046 from the National Institutes of Health (NIH), Bethesda, MD; and 14-14NSBRI1-0025 from the National Space Biomedical Research Institute (NASA). Drs. Yadava and Wu are supported by grant T32-HL094294, and Dr. Wu is also supported by grant K08-HL133493 from the NIH. Dr.s Linden and Field are supported by grant R01-HL111969 from the NIH.

The authors would like to thank Dr. Brant Isakson for his helpful comments on the manuscript.

References

1. Feigl EO. Coronary physiology. Physiological reviews. 1983; 63:1–205. [PubMed: 6296890]
2. Marcus ML, Chilian WM, Kanatsuka H, Dellsperger KC, Eastham CL, Lamping KG. Understanding the coronary circulation through studies at the microvascular level. Circulation. 1990; 82:1–7. [PubMed: 2114232]

3. Durand MJ, Gutterman DD. Diversity in mechanisms of endothelium-dependent vasodilation in health and disease. Microcirculation. 2013; 20:239–247. [PubMed: 23311975]
4. Murray CD. The physiological principle of minimum work: I. The vascular system and the cost of blood volume. Proc Natl Acad Sci U S A. 1926; 12:207–214. [PubMed: 16576980]
5. Iida K, Luo H, Hagisawa K, Akima T, Shah PK, Naqvi TZ, Siegel RJ. Noninvasive low-frequency ultrasound energy causes vasodilation in humans. J Am Coll Cardiol. 2006; 48:532–537. [PubMed: 16875980]
6. Suchkova VN, Baggs RB, Sahni SK, Francis CW. Ultrasound improves tissue perfusion in ischemic tissue through a nitric oxide dependent mechanism. Thromb Haemost. 2002; 88:865–870. [PubMed: 12428107]
7. Xie F, Lof J, Matsunaga T, Zutshi R, Porter TR. Diagnostic ultrasound combined with glycoprotein iib/iiia-targeted microbubbles improves microvascular recovery after acute coronary thrombotic occlusions. Circulation. 2009; 119:1378–1385. [PubMed: 19255341]
8. Belcik JT, Mott BH, Xie A, Zhao Y, Kim S, Lindner NJ, Ammi A, Linden JM, Lindner JR. Augmentation of limb perfusion and reversal of tissue ischemia produced by ultrasound-mediated microbubble cavitation. Circ Cardiovasc Imaging. 2015; 8:e002979. [PubMed: 25834183]
9. Siegel RJ, Suchkova VN, Miyamoto T, Luo H, Baggs RB, Neuman Y, Horzewski M, Suorsa V, Kobal S, Thompson T, Echt D, Francis CW. Ultrasound energy improves myocardial perfusion in the presence of coronary occlusion. J Am Coll Cardiol. 2004; 44:1454–1458. [PubMed: 15464327]
10. Atar S, Siegel RJ, Akel R, Ye Y, Lin Y, Modi SA, Sewani A, Tuero E, Birnbaum Y. Ultrasound at 27 khz increases tissue expression and activity of nitric oxide synthases in acute limb ischemia in rabbits. Ultrasound Med Biol. 2007; 33:1483–1488. [PubMed: 17507145]
11. Kato GJ, Hebbel RP, Steinberg MH, Gladwin MT. Vasculopathy in sickle cell disease: Biology, pathophysiology, genetics, translational medicine, and new research directions. Am J Hematol. 2009; 84:618–625. [PubMed: 19610078]
12. Wei K, Jayaweera AR, Firoozan S, Linka A, Skyba DM, Kaul S. Quantification of myocardial blood flow with ultrasound-induced destruction of microbubbles administered as a constant venous infusion. Circulation. 1998; 97:473–483. [PubMed: 9490243]
13. Pascotto M, Leong-Poi H, Kaufmann B, Allrogen A, Charalampidis D, Kerut EK, Kaul S, Lindner JR. Assessment of ischemia-induced microvascular remodeling using contrast-enhanced ultrasound vascular anatomic mapping. J Am Soc Echocardiogr. 2007; 20:1100–1108. [PubMed: 17566703]
14. Krasovitski B, Kimmel E. Shear stress induced by a gas bubble pulsating in an ultrasonic field near a wall. IEEE Trans Ultrason Ferroelectr Freq Control. 2004; 51:973–979. [PubMed: 15344403]
15. Forsyth AM, Wan J, Owrutsky PD, Abkarian M, Stone HA. Multiscale approach to link red blood cell dynamics, shear viscosity, and atp release. Proc Natl Acad Sci U S A. 2011; 108:10986–10991. [PubMed: 21690355]
16. Mortensen SP, Gonzalez-Alonso J, Bune LT, Saltin B, Pilegaard H, Hellsten Y. Atp-induced vasodilation and purinergic receptors in the human leg: Roles of nitric oxide, prostaglandins, and adenosine. Am J Physiol Regul Integr Comp Physiol. 2009; 296:R1140–1148. [PubMed: 19118095]
17. Bodin P, Bailey D, Burnstock G. Increased flow-induced atp release from isolated vascular endothelial cells but not smooth muscle cells. Br J Pharmacol. 1991; 103:1203–1205. [PubMed: 1652343]
18. Yegutkin G, Bodin P, Burnstock G. Effect of shear stress on the release of soluble ecto-enzymes atpase and 5′-nucleotidase along with endogenous atp from vascular endothelial cells. Br J Pharmacol. 2000; 129:921–926. [PubMed: 10696091]
19. Coade SB, Pearson JD. Metabolism of adenine nucleotides in human blood. Circ Res. 1989; 65:531–537. [PubMed: 2548757]
20. Burnstock, G., Verkhratsky, A. Mechanisms of atp release and inactivation. In: Burnstock, G., Verkhratsky, A., editors. Purinergic signalling and the nervous system. Berlin, Germany: Springer-Verlag; 2012. p. 79-118.
21. Ray CJ, Marshall JM. The cellular mechanisms by which adenosine evokes release of nitric oxide from rat aortic endothelium. The Journal of physiology. 2006; 570:85–96. [PubMed: 16239264]

22. Duza T, Sarelius IH. Conducted dilations initiated by purines in arterioles are endothelium dependent and require endothelial ca2+ Am J Physiol Heart Circ Physiol. 2003; 285:H26–37. [PubMed: 12637357]

23. Ansari HR, Nadeem A, Talukder MA, Sakhalkar S, Mustafa SJ. Evidence for the involvement of nitric oxide in a2b receptor-mediated vasorelaxation of mouse aorta. Am J Physiol Heart Circ Physiol. 2007; 292:H719–725. [PubMed: 16920807]

24. Wall MJ, Wigmore G, Lopatar J, Frenguelli BG, Dale N. The novel ntpdase inhibitor sodium polyoxotungstate (pom-1) inhibits atp breakdown but also blocks central synaptic transmission, an action independent of ntpdase inhibition. Neuropharmacology. 2008; 55:1251–1258. [PubMed: 18768144]

25. Erga KS, Seubert CN, Liang HX, Wu L, Shryock JC, Belardinelli L. Role of a(2a)-adenosine receptor activation for atp-mediated coronary vasodilation in guinea-pig isolated heart. Br J Pharmacol. 2000; 130:1065–1075. [PubMed: 10882391]

26. Liu C, Mather S, Huang Y, Garland CJ, Yao X. Extracellular atp facilitates flow-induced vasodilatation in rat small mesenteric arteries. Am J Physiol Heart Circ Physiol. 2004; 286:H1688–1695. [PubMed: 14715503]

27. Ralevic V, Burnstock G. Receptors for purines and pyrimidines. Pharmacological reviews. 1998; 50:413–492. [PubMed: 9755289]

28. Crecelius AR, Kirby BS, Richards JC, Garcia LJ, Voyles WF, Larson DG, Luckasen GJ, Dinenno FA. Mechanisms of atp-mediated vasodilation in humans: Modest role for nitric oxide and vasodilating prostaglandins. Am J Physiol Heart Circ Physiol. 2011; 301:H1302–1310. [PubMed: 21784984]

29. da Silva CG, Specht A, Wegiel B, Ferran C, Kaczmarek E. Mechanism of purinergic activation of endothelial nitric oxide synthase in endothelial cells. Circulation. 2009; 119:871–879. [PubMed: 19188511]

30. Xing M, Post S, Ostrom RS, Samardzija M, Insel PA. Inhibition of phospholipase a2-mediated arachidonic acid release by cyclic amp defines a negative feedback loop for p2y receptor activation in madin-darby canine kidney d1 cells. J Biol Chem. 1999; 274:10035–10038. [PubMed: 10187781]

31. Jiang JG, Chen RJ, Xiao B, Yang S, Wang JN, Wang Y, Cowart LA, Xiao X, Wang DW, Xia Y. Regulation of endothelial nitric-oxide synthase activity through phosphorylation in response to epoxyeicosatrienoic acids. Prostaglandins other lipid mediat. 2007; 82:162–174. [PubMed: 17164144]

32. Lindner JR, Song J, Jayaweera AR, Sklenar J, Kaul S. Microvascular rheology of definity microbubbles after intra-arterial and intravenous administration. J Am Soc Echocardiogr. 2002; 15:396–403. [PubMed: 12019422]

33. Wan J, Ristenpart WD, Stone HA. Dynamics of shear-induced atp release from red blood cells. Proc Natl Acad Sci U S A. 2008; 105:16432–16437. [PubMed: 18922780]

34. Sprague RS, Ellsworth ML, Stephenson AH, Kleinhenz ME, Lonigro AJ. Deformation-induced atp release from red blood cells requires cftr activity. Am J Physiol. 1998; 275:H1726–1732. [PubMed: 9815080]

35. Sridharan M, Adderley SP, Bowles EA, Egan TM, Stephenson AH, Ellsworth ML, Sprague RS. Pannexin 1 is the conduit for low oxygen tension-induced atp release from human erythrocytes. Am J Physiol Heart Circ Physiol. 2010; 299:H1146–1152. [PubMed: 20622111]

36. Meijering BD, Juffermans LJ, van Wamel A, Henning RH, Zuhorn IS, Emmer M, Versteilen AM, Paulus WJ, van Gilst WH, Kooiman K, de Jong N, Musters RJ, Deelman LE, Kamp O. Ultrasound and microbubble-targeted delivery of macromolecules is regulated by induction of endocytosis and pore formation. Circ Res. 2009; 104:679–687. [PubMed: 19168443]

37. Secomb TW, Pries AR. Blood viscosity in microvessels: Experiment and theory. Comptes rendus Physique. 2013; 14:470–478. [PubMed: 25089124]

38. Ryu JC, Davidson BP, Xie A, Qi Y, Zha D, Belcik JT, Caplan ES, Woda JM, Hedrick CC, Hanna RN, Lehman N, Zhao Y, Ting A, Lindner JR. Molecular imaging of the paracrine proangiogenic effects of progenitor cell therapy in limb ischemia. Circulation. 2013; 127:710–719. [PubMed: 23307829]

39. Richards JP, Yosten GL, Kolar GR, Jones CW, Stephenson AH, Ellsworth ML, Sprague RS. Low o2-induced atp release from erythrocytes of humans with type 2 diabetes is restored by physiological ratios of c-peptide and insulin. Am J Physiol Regul Integr Comp Physiol. 2014; 307:R862–868. [PubMed: 25080497]
40. Ellsworth ML, Forrester T, Ellis CG, Dietrich HH. The erythrocyte as a regulator of vascular tone. Am J Physiol. 1995; 269:H2155–2161. [PubMed: 8594927]
41. Lockwood SY, Erkal JL, Spence DM. Endothelium-derived nitric oxide production is increased by atp released from red blood cells incubated with hydroxyurea. Nitric oxide. 2014; 38:1–7. [PubMed: 24530476]
42. Xie F, Slikkerveer J, Gao S, Lof J, Kamp O, Unger E, Radio S, Matsunaga T, Porter TR. Coronary and microvascular thrombolysis with guided diagnostic ultrasound and microbubbles in acute st segment elevation myocardial infarction. J Am Soc Echocardiogr. 2011; 24:1400–1408. [PubMed: 22037348]
43. Leybaert L, Sanderson MJ. Intercellular ca(2+) waves: Mechanisms and function. Physiological reviews. 2012; 92:1359–1392. [PubMed: 22811430]
44. Locovei S, Wang J, Dahl G. Activation of pannexin 1 channels by atp through p2y receptors and by cytoplasmic calcium. FEBS letters. 2006; 580:239–244. [PubMed: 16364313]
45. Juffermans LJ, van Dijk A, Jongenelen CA, Drukarch B, Reijerkerk A, de Vries HE, Kamp O, Musters RJ. Ultrasound and microbubble-induced intra- and intercellular bioeffects in primary endothelial cells. Ultrasound Med Biol. 2009; 35:1917–1927. [PubMed: 19766381]
46. Leinenga G, Gotz J. Scanning ultrasound removes amyloid-beta and restores memory in an alzheimer's disease mouse model. Sci Transl Med. 2015; 7:278ra233.
47. Xie A, Belcik T, Qi Y, Morgan TK, Champaneri SA, Taylor S, Davidson BP, Zhao Y, Klibanov AL, Kuliszewski MA, Leong-Poi H, Ammi A, Lindner JR. Ultrasound-mediated vascular gene transfection by cavitation of endothelial-targeted cationic microbubbles. JACC Cardiovasc Imaging. 2012; 5:1253–1262. [PubMed: 23236976]

CLINICAL PERSPECTIVE

What is New?

- Ultrasound together with microbubble (MB) contrast agents can markedly augment limb by several fold through a mechanism that involves vascular shear during MB cavitation.
- This flow augmentation relies on local release of ATP which mediates vasodilation through direct purinergic signaling to increase production of nitric oxide and prostanoids, and through ectonucleotidase conversion to adenosine.
- Augmentation of perfusion with ultrasound and MBs extends well beyond the region insonified and can reverse limb ischemia in mice for >24 hrs, and improve skeletal muscle perfusion in patients with sickle cell disease

What are the Clinical Implications?

- Ultrasound cavitation of MBs represents a promising approach for rapidly correcting tissue perfusion in acute ischemic syndromes or for treating chronic ischemic symptoms.
- Cavitation-related release of ATP may serve to explain ultrasound's role in other therapeutic applications such as wound and bone healing, and ultrasound-facilitated drug or gene uptake.
- The shear- and endothelial-dependent pathways activated by MB cavitation indicate that this approach could potentially be used to assess endothelial vasodilator function.

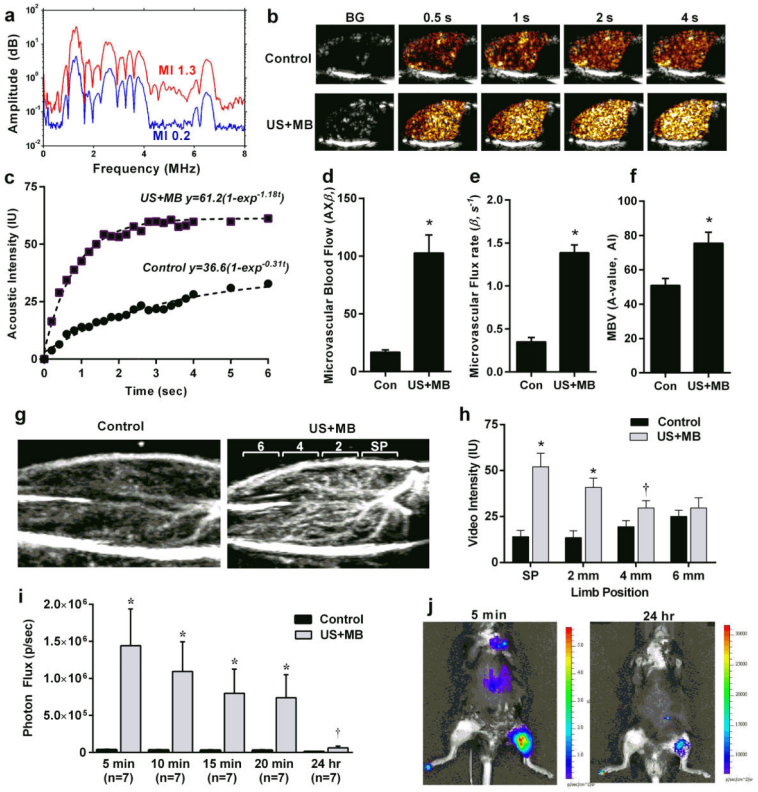

Figure 1. Release of ATP by US Cavitation

(**a**) Passive cavitation detection obtained from the mouse hindlimb during US (1.3 MHz) exposure of intravenously-infused MBs. Inertial cavitation is indicated by the broad-band signal between the harmonic peaks seen at a mechanical index of 1.3 but not at 0.2. (**b**) Examples of frames obtained during low-power CEU perfusion imaging from the proximal hindlimb adductor muscles and (**c**) corresponding time-intensity data obtained from a control (non-US-exposed) and an US-exposed limb illustrating greater blood flow in the latter (*BG* = background). Data were obtained 10 min after exposure to high-power US for 10 min during intravenous MB infusion. (**d**) Microvascular blood flow and (**e**) microvascular flux rate, and (**f**) microvascular blood volume (*MBV*) (mean ±SEM) in the contralateral control (*Con*) and US-exposed (*US+MB*) hindlimbs of mice obtained 10 min after therapeutic US; *p<0.01. (**g** and **h**) Examples of CEU of the proximal hindlimb with maximal intensity projection in the long-axis, and mean (±SEM) intensity from the control and US-exposed (*US+MB*) limbs. Imaging was performed with a 90-degree rotation from therapeutic US plane 10 min after therapeutic US and illustrates distribution of perfusion within the 2 mm-wide therapeutic US sector plane (*SP*) and distal adjacent sectors at 2, 4, and 6 mm increments. *p<0.01 vs control limb; †p=0.05 versus control. (**i**) *In vivo* optical imaging of intravascular ATP release by luciferin-luciferase activity in contr and US-exposed (*US+MB*) limbs. Data were obtained at various intervals after completing a 10 min US exposure during MB infusion. *p<0.001 vs control; †p<0.05 versus control. (**j**) Examples of optical imaging illustrating focal ATP production at the site of US cavitation (left proximal hindlimb).

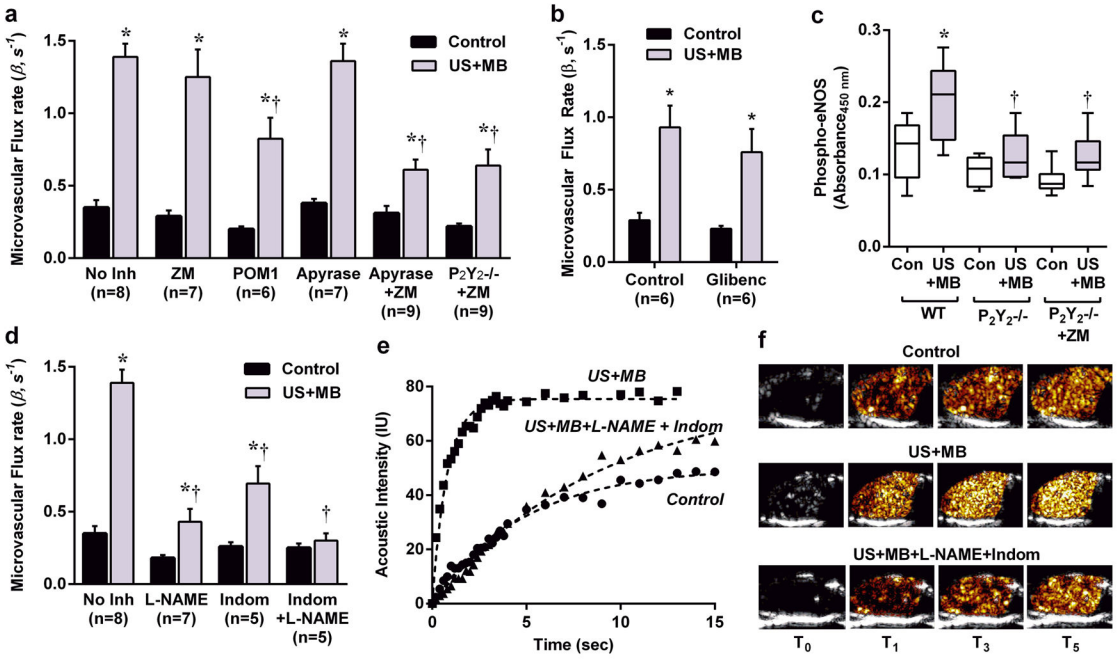

Figure 2. Mechanism of Muscle Flow Augmentation During US Cavitation

(**a**) Mean (±SEM) microvascular flux rate in contralateral control and US-exposed (*US +MB*) limbs in wild-type control mice without inhibitors (*No Inh*); in wild-type mice pre-treated with inhibitors to vasoactive pathways (see text); and in $P2Y_2^{-/-}$ mice treated with the adenosine A_{2a} receptor antagonist ZM241385 (*ZM*). *p<0.05 vs control; †p<0.05 versus no inhibitor. (**b**) Mean (±SEM) microvascular flux rate in contralateral control and US-exposed limbs in wild-type mice with and without pre-treatment with glibenclamide; *p<0.05 versus untreated control limb; p=ns between control and glibenclamide groups. (**c**) Skeletal muscle phosphorylated eNOS by ELISA from control and US cavitation-exposed legs in wild-type (WT) (n=9), $P2Y_2^{-/-}$ (n=5), and $P2Y_2^{-/-}$ ZM-treated (n=6) mice. *p<0.05 vs control limb; †p<0.05 versus corresponding wild-type US+MB conditions. (**d**) Mean (±SEM) microvascular flux rate in control and US-exposed limbs in wild-type mice in mice pre-treated with L-NAME, indomethacin, or L-NAME and indomethacin. *p<0.05 vs. control; †p<0.0001 versus no inhibitor. (**e**) Examples of time-intensity curves and (**f**) selected source CEU perfusion images from variable times (t_{sec}) after the destructive frame from a control limb, and limbs exposed to US+MB with and without L-NAME +indomethacin treatment.

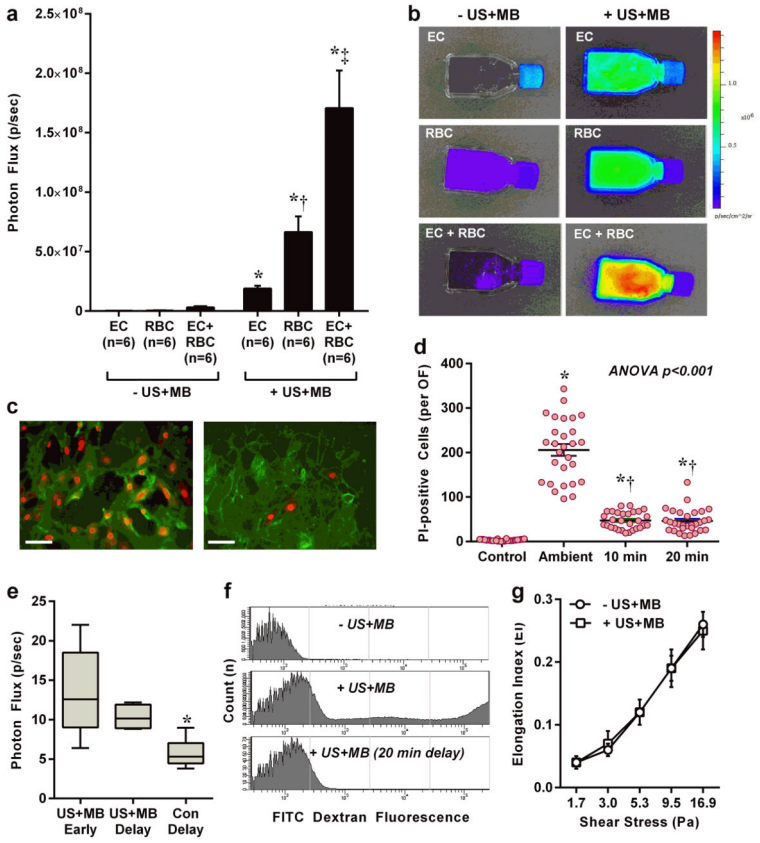

Figure 3. Cellular Sources of ATP Release During MB Cavitation

(**a** and **b**) Optical imaging data (mean ±SEM) and examples of ATP release detected by luciferin-luciferase activity from cultured endothelial cells (*EC*), human RBCs, and the combination of ECs with RBCs. Data are from control (− *US+MB*) and US-exposed (+ *US +MB*) conditions. *p<0.01 vs corresponding control conditions (−US+MB); †p<0.05 vs EC; ‡p<0.01 vs EC and RBC. (**c**) Fluorescent microscopy illustrating di-I-stained ECs (green) with positive nuclear propidium iodide (*PI*) staining (red) which was much more extensive when PI was ambient at the time of MB cavitation (*left*) than when PI was added after a 20 min delay (*right*). Scale bar = 25 μm. (**d**) Number of cells per optical field (OF) with positive nuclear staining when PI was ambient at the time of MB cavitation, or was added after 10 or 20 min delay. *p<0.0001 vs control; †p<0.001 vs ambient. (**e**) ATP activity from endothelial cells without and with a 20 delay in adding luciferin and luciferase with interval medium exchange. Control conditions with medium exchange alone are also shown. (**f**) Flow cytometry of RBCs exposed to FITC dextran without cavitation (− US+MB), or with cavitation (+ US+MB). The center histogram illustrates the presence of fluorescent RBCs from microporation which was not seen when FITC dextran was added 20 min after US (bottom). (**g**) RBC deformability expressed as the elongation index at various shears for RBCs exposed to US and MBs and for control RBCs.

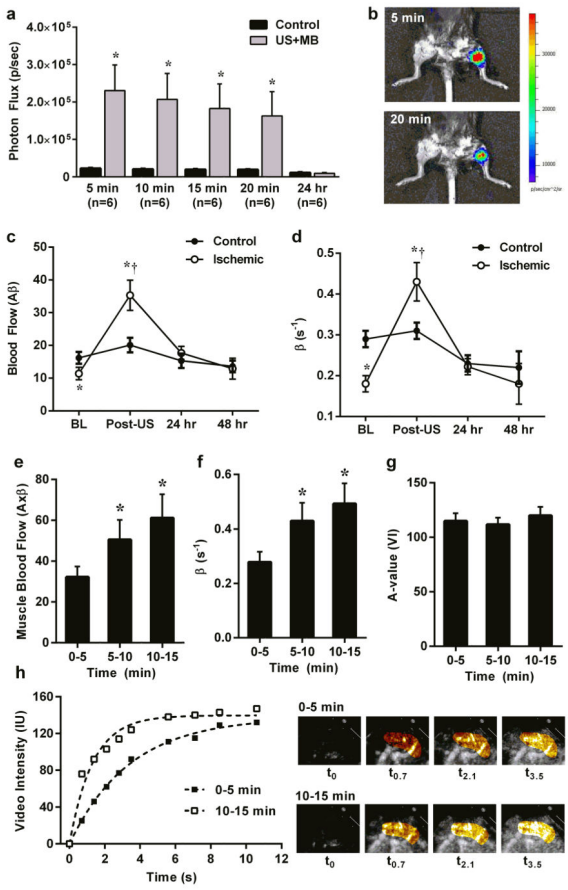

Figure 4. Therapeutic Response to US Cavitation

(**a**) In vivo optical imaging of luciferase activity (mean ±SEM) in ischemic control and US-exposed (*US+MB*) limbs obtained at various intervals after completing a 10 min US exposure during MB infusion. *p<0.01 vs control. (**b**) Example illustrating focal luciferase activity at the site of US exposure (proximal hindlimb). (**c**) Microvascular blood flow and (**d**) microvascular flux rate from skeletal muscle in ischemic and control limbs at baseline (*BL*) and immediately after (Post-US), 24 hr, and 48 hr after exposure of the ischemic limb to US and MBs. *p<0.01 vs control; †p<0.01 versus baseline. (**e**) Microvascular blood flow, (**f**) microvascular flux rate, and (**g**) microvascular blood volume measured from the proximal forearm flexor muscles in patients with SCD. Data are shown at various times after starting US exposure during a continuous infusion of MBs. *p≤0.01 versus 0–5 min. (**h**) Example of time-intensity data and source background-subtracted color-coded CEU images from the forearm of a patient with SCD illustrating an increase in muscle perfusion with increasing time of cavitation exposure.

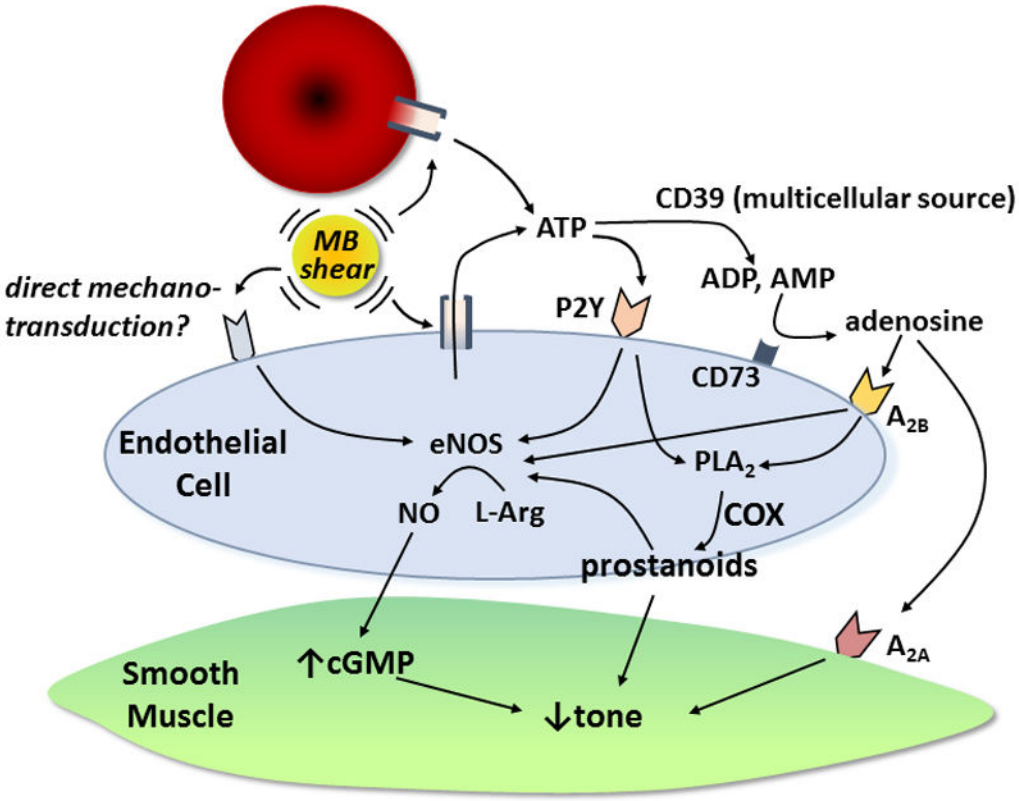

Figure 5. Schematic Illustrating Pathways Responsible for Increases in Skeletal Muscle Blood Flow Produced by US-mediated MB Cavitation

COX, cyclooxygenase. L-Arg, L-arginine.